

Abscisic acid affects the floret numbers of inflorescence by regulating indole-3-acetic acid transport and accumulation in *Lavandula angustifolia*

H.P. HAO^{1,3,+}, Y.M. DONG^{1,2,+}, X.P. ZHU⁴, H.T. BAI¹, H.LI¹, J. GONG⁵, A. FAROOQ⁶, L. SHI^{1*} 

¹Institute of Botany, Chinese Academy of Sciences, Xiangshan, Beijing 100093, P.R. China

²University of Chinese Academy of Sciences, Beijing 100049, P.R. China

³Lang Fang Normal University, Lang Fang 065000, HeBei, P.R. China

⁴Henan Institute of Science and Technology, Xinxiang, Henan Province, 453003, P.R. China

⁵Agricultural School of Handan City, Handan City, 056001, P.R. China

⁶Department of Environmental Sciences, COMSATS University Islamabad, Vehari Campus 61100, Pakistan

*Corresponding author: E-mail: shilei@ibcas.ac.cn

Abstract

Lavender flower essential oil had been used for a variety of therapeutic and cosmetic purposes. Previous studies mainly focused on essential oil composition and extraction methods, ignoring the factors that affected the production of essential oils, such as the floret number. This study aims to get a deep insight into the mechanism of floret number differences. Hormone analysis showed that there was a positive correlation between abscisic acid (ABA) content and the number of florets, while indole-3-acetic acid (IAA) was negatively correlated with floret numbers. RNA-Seq results showed that 1 035 differentially expressed genes (DEG) can be identified, of which 19 genes were significantly enriched in the carotenoid biosynthesis pathway. Common network analysis showed that the expression of the key genes of ABA pathway metabolism was negatively related to the DEG of IAA, especial *IAA18*. Exogenous IAA significantly inhibited the number of lavender florets and affected the expression of ABA metabolism genes. The results might be useful for a better understanding of the molecular mechanism of floret number differences.

Keywords: abscisic acid, branching, florets number, indole-3-acetic acid, inflorescence, *Lavander angustifolia*.

Introduction

Lavender belonging to the family *Lamiaceae* have been used as dried flowers and for extracting essential oil which is used for a variety of therapeutic and cosmetic purposes for long time (Zai 2011). Lavender essential oil is extracted from both the flowers and foliage by steam distillation with varying chemical composition, but most of the aromatic oil is derived from the flowers (Li *et al.* 2019). Lavender inflorescence is a discontinuous or almost continuous

clusters of cymes growing on the top of branches. One lavender plant has about 100 branches, and the number of florets of each branch is variable, and the difference between the maximum and minimum number is about 2.5 times. The numbers of florets affect the ornamental value, the quality of dried flowers and the yield of essential oils, which determines the economic benefits of lavender planting. Therefore, it is of great significance to study the difference in the number of florets.

Inflorescence architectures directly affect the number of

Received 5 March 2022, last revision 19 July 2022, accepted 28 July 2022.

Abbreviations: ABA - abscisic acid; BCH - β -carotene hydroxylase; BM - branch meristem; DEG - differentially expressed genes; FM - floral meristems; GA - gibberellic acid; IAA - indole-3-acetic acid; IM - inflorescence meristem; NCED - 9-*cis*-epoxycarotenoid dioxygenase; PP2C - type 2c protein phosphatase; PYL - pyrabactin resistance-like ABA receptor; SAM - shoot apical meristem; SM - spikelet meristem; SnRK2 - sucrose non-fermenting 1-related protein kinase 2; ZR - zeatin riboside.

Acknowledgements: We thank An-Yang (Institute of Botany, CAS) and Xiu Qing Li (Agriculture and Agri-Food Canada, Potato Research Centre) for thoughtful feedback and discussions on manuscript. We also thanks for the funding of the key deployment projects of Chinese Academy of Sciences (No. Y7612G1001), Chinese National Natural Science Foundation (No. Y8628A1001), and Lang Fang Normal University Science Foundation (No. XBQ202030).

Conflict of interest: No competing interests declared.

Database accession NCBI number PRJNA850545. ⁺These authors contributed equally.

florets. The aerial organs of plant come from the shoot apical meristem (SAM) which transforms into the inflorescence meristem (IM) after the floral transition. The key parameter affects the structure of the inflorescence is whether the IM ends in a terminal flower (determinate) or continues to produce branches and flowers (indeterminate). In the type of cymes inflorescence, the IM gives rise to several branch meristems (BM_s, which are usually indeterminate meristems). These BMs may initiate secondary BMs to form lateral branches and spikelet meristems (SMs) that then initiate floral meristems (FMs) (Han *et al.* 2014). Meristem activity, especially determinacy, fundamentally affects inflorescence architecture and floret numbers. Previous studies showed that the meristems activity of IM_s and BMs in inflorescences that branch interactively, and the indeterminate lateral meristem formation in inflorescences that branch laterally are likely to be related to plant hormones, of which indole-3-acetic acid (IAA), cytokinins, strigolactone, and abscisic acid (ABA) are particularly important (Ongaro and Leyser 2008, McSteen 2009).

The IAA was the first hormone to be linked to the regulation of meristem activity and it has been in the spotlight for more than 100 years. As suggested by the analysis of several auxin biosynthetic mutants in different species including *Arabidopsis*, petunia, maize, and rice, auxin biosynthesis is required for the formation of all primordia, including SAM, IM, BM, and FM (Cheng *et al.* 2007). The study on inflorescence development in maize showed that the polar auxin transport mechanism is necessary for the formation of all axillary meristems and lateral primordia in maize, similarly as in *Arabidopsis* (Cheng *et al.* 2007). Defective auxin transport, caused by either chemical transport inhibitors or specific genetic mutations, affects organogenesis and the formation of all primordia, including new axillary meristems (Wu and McSteen 2007, Xie *et al.* 2021).

Cytokinins can promote inflorescence complexity in different ways, by promoting the meristem activity of IMs and BMs in inflorescences that branch interactively, and by promoting the indeterminate lateral meristem formation in inflorescences that branch laterally (Han *et al.* 2014). Strigolactones blocked the transport of IAA through the Pin protein to regulate branching (Ferguson and Beveridge 2009). The ABA likewise inhibited the expression of genes associated with the IAA biosynthesis pathway and hindered the transport and accumulation of IAA (Yao and Finlayson 2015, Emenecker and Strader 2020). ABA and IAA cross-talk has a regulatory effect on a variety of plant developmental processes, such as seed vigor, lateral root formation, axillary-bud outgrowth, apical dominance, *etc.* However, there are few reports on the regulation of floret numbers (Yao and Finlayson 2015, Murphy 2015, He *et al.* 2020). The number of florets was a key factor affecting agricultural yields and benefits, so it is necessary to conduct in-depth research.

In *Lavander angustifolia* cv. JX-2, all inflorescences had five whole flowers but the floret number of different inflorescence varies from 30 to 70, and the reason for differences in floret numbers was poorly understood. In this

study, we aimed to understand floret numbers differences in *L. angustifolia* by addressing the following issues: 1) what hormones regulate the number of florets; 2) what are the key genes in metabolic pathways that affect floret number; and 3) what is possible regulatory mechanism of the difference in floret numbers.

Materials and methods

Plants: In the lavender planting area of 65th group farm in Xin Jiang, 667 m² was selected as experimental area. In the experimental area, 3-year-old lavender (*Lavander angustifolia* L. cv. JX-2) plants were selected as the sample plants, 10 plants were used as one group and 3 replicates were used. The flowering branches with 6 florets (LaF6), 10 florets (LaF10), and 14 florets (LaF14) per round in bud stage of each sample plants were used as experimental materials. The flowering branches with different florets were divided into four parts: florets, floral axis 1, floral axis 2, and floral axis leaf (Fig. 1 Suppl.). Ten LaF6, LaF10, and LaF14 flowering branches from 10 sample plants were mixed thoroughly, then weighed, packed, immediately frozen in liquid nitrogen, and stored at -80 °C until use. The three replicates were sampled in the same way.

Indole-3-acetic acid application: Consistent JX-2 seedlings were selected for IAA treatment. The concentrations of IAA were 300 and 800 mg dm⁻³, respectively, and the control was 0.1 % ethanol + distilled water. There were 5 pots of seedlings per treatment, and each treatment has 3 replicates. Spray was performed once every 7 d and 5 times continuously. After the flower buds were formed, the floral axis leaves were taken from the flower branches put into the ziplock bag which filled with ice bag, and brought into the laboratory, then were weighed, packed and immediately frozen in liquid nitrogen and stored at -80 °C. Then RNA extraction and reverse transcription quantitative PCR (RT-qPCR) were performed to examine the expression of ABA metabolism pathway genes.

Hormone determination: The content of gibberellic acid (GA), ABA, IAA, cytokinin zeatin riboside (ZR) of four parts (florets, floral axis 1, floral axis 2, floral axis leaf) for LaF6, LaF10, and LaF14 samples were measured. Firstly, hormones were extracted and purified from 0.5 g of each sample. Secondly, the extracted hormone elution was analyzed according to the enzyme-linked immunosorbent assay (ELISA) method described by the previous study (Yang *et al.* 2001). The mouse monoclonal antigens and antibodies against GA, ABA, IAA, ZR, and immunoglobulin G-horseradish peroxidase (IgG-HRP) used in the ELISA were produced at the Phytohormones Research Institute, China Agricultural University, Beijing, China. In order to exclude the influence of the difference in leaf water status on GA, ABA, IAA, ZR content, and all hormone content was expressed on a leaf dry mass basis.

Gas chromatography-mass spectrometry (GC-MS):

0.5 g of each floral axis leaf samples were used for the determination of ABA and IAA content with 3 replicates. The modified GC-MS was used for accurate determination of hormone content as previously described (Müller *et al.* 2002).

The internal standard [$^2\text{H}_6$] ABA was purchased from *OlChemIm Company* (Olomouc, Czech Republic) and [$^{13}\text{C}_6$] IAA was purchased from *Cambridge Isotope Laboratories* (Cambridge, UK).

RNA isolation and cDNA library construction for Illumina sequencing: Total RNA of each sample was obtained using an *RNAprep Pure Plant* kit (*Tiangen Biotech*, Beijing, China) according to the manufacturer's instructions. The quality of RNA was determined using the *NanoDrop 1000* spectrophotometer and *Agilent 2100* bioanalyzer (*Agilent Technologies*, Santa Clara, USA), and the RNA integrity number (RIN) value of all sequencing samples was more than 8.0. The cDNA libraries were constructed as described below. Total RNA of each sample was treated with DNase I, and poly (A) mRNA was then isolated with oligodT beads, followed by reverse-transcription into first-strand cDNA using reverse transcriptase. Second-strand cDNA was synthesized using DNA polymerase I and RNaseH, and then ligated with an adaptor of index adaptor using T4 DNA ligase. Adaptor-ligated fragments were separated and excised by agarose gel electrophoresis. PCR was performed to selectively enrich and amplify the cDNA fragments. Finally, the cDNA libraries were sequenced using *Illumina HiSeq 3000* at *Novogene Tech Solutions Co.* (Tianjin, China).

De novo assembly and functional annotation: Adaptor sequences, reads with unknown sequences, and low-quality reads were removed and the clean reads were then assembled using *Trinity* software (Grabherr *et al.* 2011). Data obtained for each sample were separately assembled and the assembly sequences were called unigenes. The unigenes from all samples were further subjected to sequence splicing and redundancy removal with sequence clustering software to acquire non-redundant unigenes as long as possible. These unigene sequences were aligned and annotated to protein databases like *Nr*, *Swiss-Prot*, *PFAM*, *COG* (Tatusov *et al.* 2001), *GO* (Conesa *et al.* 2005), *KO* (Kanehisa *et al.* 2012), and nucleotide database *Nt* with a threshold of $E < 10^{-5}$. The best aligning results were used to decide sequence direction of unigenes. If results from different databases conflicted with each other, a priority order of *Nr*, *Swiss-Prot*, *KEGG* and *COG* should be followed.

Analysis of differentially expressed genes (DEGs): Expression of the unigenes was calculated using the FPKM (fragments per kb per million reads) which eliminated the influence of lengths and sequencing discrepancies of different genes on the gene expression calculations. DEGs were selected on condition of Q value < 0.005 and an absolute value of $|\log_2\text{FoldChange}| \geq 2$.

Quantitative real-time PCR validation: Total RNA was

separately extracted from floral axis leaf for LaF6, LaF10, and LaF14 samples as described earlier. First-strand cDNA was synthesized using the *PrimeScript® RT* reagent kit (*Takara*, Dalian, China) according to the manufacturer's instructions. The primers for the selected genes were designed using *Primer Premier 5.0* software. The qRT-PCR was performed using the *Power SYBR Green PCR Master Mix* on the *StepOne Plus* Real time PCR Platform (*Applied Biosystems*, USA). This experiment was carried out with the following procedure: 95 °C for 10 min, followed by 40 cycles of 95 °C for 15 s, and 60 °C for 60 s. The correlation between the results of RNA-seq and RT-qPCR were evaluated using R^2 value.

Statistical analysis: ANOVA and Dennett's tests were used to determine the ABA content among different floret samples, statistical significance were expressed at $P \leq 0.05$ and $P \leq 0.01$ (*SPSS 11.0*, Chicago, IL, USA). Mean values and standard deviations (SD) were obtained from three replicates. The correlation between DEGs of ABA and IAA was assessed by two-way analysis of variance using the software of *SPASS 11.0*.

Results

The botanical characteristics of lavender were dwarf shrubs, branch with long inflorescence. One three-year-old plant had about 100 flowering branches (Fig. 1A). Each flowering shoots borne five whorl flowers (Fig. 1B). Take one side of one round flower for example, the 2nd flower had symmetry but the flowers begun to be inward hyperplasia from the third flower (Fig. 1C). The inflorescence of lavender cv. JX-2 was 30 - 70 flowers per shoots, 6 - 14 florets per round (Fig. 1B).

The hormone content of different parts in LaF6, LaF10, and LaF14 samples were measured by ELISA (Table 1 Suppl.). The hormone content of florets and flower axis 1 were not significantly different. In flower axis leaf and flower axis 2, the change trends of GA and ZR content were similar, while the ABA and IAA content of flower axis leaf in three samples had the big differences (Table 1 Suppl.). The ABA content was the lowest in LaF6 sample, followed by that in the LaF10, and highest in the LaF14. However, for IAA, flower axis leaf from LaF6 sample had the highest content followed by that in LaF10 and the lowest in the LaF14. Further evidence from GC-MS supported the result that the ABA content of flower axis leaf from sample with more floret numbers was higher; while IAA was lower (Fig. 2A). The ABA/IAA ratio also increased along with the increase in the floret numbers, and the ABA/IAA ratio of LaF14 was the highest among them (Fig. 2B).

The three cDNA samples were prepared from floral axis leaf of the LaF6, LaF10, and LaF14 samples and sequenced using the *Illumina HiSeq 3000*. After stringent quality check and data cleaning, 6.17 - 7.67 GB clean nucleotides were obtained for each sample, totaling 20.45 GB nucleotides for all samples (Table 2 Suppl.). The Q20 (sequencing error rate $< 1\%$) and guanine-

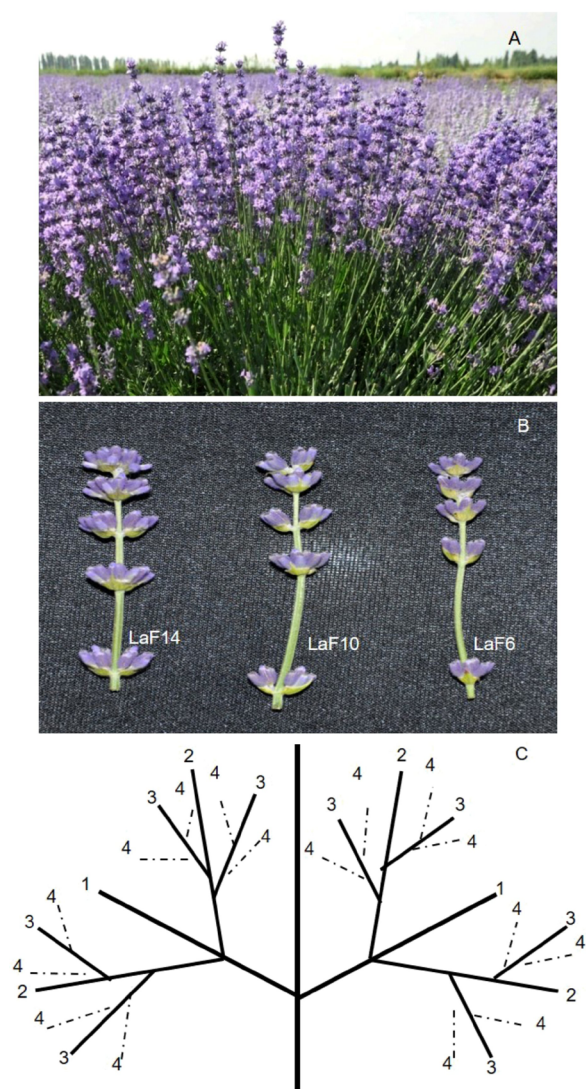


Fig. 1. The lavender characteristic inflorescences and schematic diagram of floret. *A* - inflorescence clusters of lavender, *B* - inflorescences of different florets; LaF6 - 6 florets per flower whorl, LaF10 - 10 florets per flower whorl, LaF14 - 14 florets per flower whorl, *C* - schematic line diagram of florets in a complete whorl, the dotted line indicates the theoretical number of florets, the solid line indicates the number of florets that can be birthed in production.

cytosine (GC) content were 96.21 - 96.95 % and 47.75 - 48.17 %, respectively (Table 2 Suppl.). The completeness of transcriptome data was checked by *BUSCO*: complete 72.96 %; partial 12.82 %; missing, 14.22 % (Fig. 2 Suppl.).

All unigenes were aligned to six protein databases including *Nr*, *KO*, *PFAM*, *Swiss-Prot*, *GO*, and *KOG*. A total of 103 555 unigenes were annotated which contained 72 820 (70.32 %) unigenes identified from *Nr*, 52 114 (50.32 %) from *Nt*, 30 814 (29.75 %) from *KO*, 57 472 (55.50 %) from *Swiss-Prot*, 51 664 (49.89 %) from *PFAM*, 51 985 (50.2 %) from *GO*, and 32 247 (31.14 %) from *KOG* (Table 3 Suppl.). E-value indicated the extent of sequence homology and if E-value is smaller, the sequence homology is higher. For E-value distribution of unigenes,

BLASTX hits in the *Nr* database which had the largest number of annotated unigenes, 37 % homolog sequences ranged between $1E^{-5}$ to $1E^{-60}$, while 63 % sequence had a threshold E-value less than $1E^{-60}$ which showed strong homology (Fig. 3A Suppl.). Species distribution of the first *BLASTX* hits of each unigene in the *Nr* database indicated that *Sesamum indicum* provided the best matches with 56.8 % unigenes in lavender, and *Erythranthe guttata* was the second closest species, which had 13.8 % homology with lavender (Fig. 3B Suppl.).

To gain insight into the functions of the annotated genes from the macro level, *GO* functional classification was performed. A total of 55 *GO* terms were categorized into three domains: biological processes, cellular components, and molecular functions (Fig. 4 Suppl.). The term of 'cellular process', 'metabolic process' and 'single-organism process'; 'cell' and 'cell part'; 'binding' and 'catalytic activity' were the most representative of biological processes, cellular component and molecular function, respectively (Fig. 4 Suppl.).

KEGG mapping of all the unigenes was carried out to analyze the pathways involved in lavender transcriptome and 131 pathways were identified. The 'translation' had the greatest number of members, followed by 'carbohydrate metabolism' and 'folding, sorting and degradation' (Fig. 5 Suppl.). *KOG* analysis was performed to predict phylogenetic classification. In total, 36 062 unigenes were matched and were grouped into 25 functional classes, the clusters for 'general function prediction only' and 'posttranslational modification, protein turnover, chaperones' were the two largest groups (Fig. 7 Suppl.).

With Q value < 0.005 and an absolute $|\log_2\text{FoldChange}| \geq 2$, a total of 1 035 genes were found to be differently expressed among the groups LaF6 vs. LaF10, LaF6 vs. LaF14, and LaF10 vs. LaF14. In the group LaF6 vs. LaF10, 607 genes were found, among which 355 genes were down-regulated and 252 genes were up-regulated. In the LaF6 vs. LaF14 group, 723 genes were differently expressed, of which 341 genes were up-regulated and 382 genes were down-regulated. In LaF10 vs. LaF14 group, 170 genes were up-regulated and 163 genes were down-regulated (Fig. 3A). These results indicated that the transcript abundance of genes changed dynamically among the different floret samples.

To validate DEGs expression profiling obtained by RNA-seq, 7 DEGs in LaF10 vs. LaF14 group, 17 DEGs in LaF6 vs. LaF14 group and 12 DEGs in LaF6 vs. LaF10 group were selected for RT-qPCR analysis, and their expression trends were similar to that in RNA-Seq. Their correlation coefficients (R^2) ranged from 0.94 to 0.97, which was very significant ($P < 0.01$) (Fig. 3B-D). Thus, data from RNA-Seq in this study were reliable.

To further understand the mechanism of floret number differences on inflorescence at the molecular level in *L. angustifolia*, we mapped the DEGs to the terms in the *KEGG* database, The top 20 *KEGG* pathway was photosynthesis, carbon fixation in photosynthetic organisms, nitrogen metabolism, plant hormone signal transduction, carotenoid biosynthesis, etc., and the hormone metabolism and transduction pathway was one of

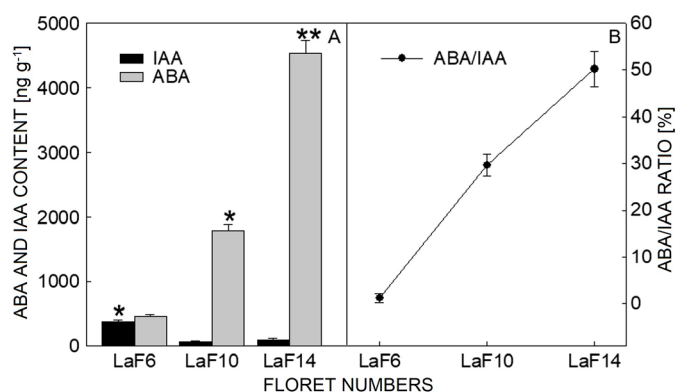


Fig. 2. ABA, IAA content and the ABA/IAA in flower axis leaf. *A* - ABA and IAA content, *B* - ABA/IAA ratio. Means \pm SEs, $n = 3$; *, ** significantly different values at $P \leq 0.05$ and 0.001 , respectively. LaF6 - 6 florets per flower whorl, LaF10 - 10 florets per flower whorl, LaF14 - 14 florets per flower whorl.

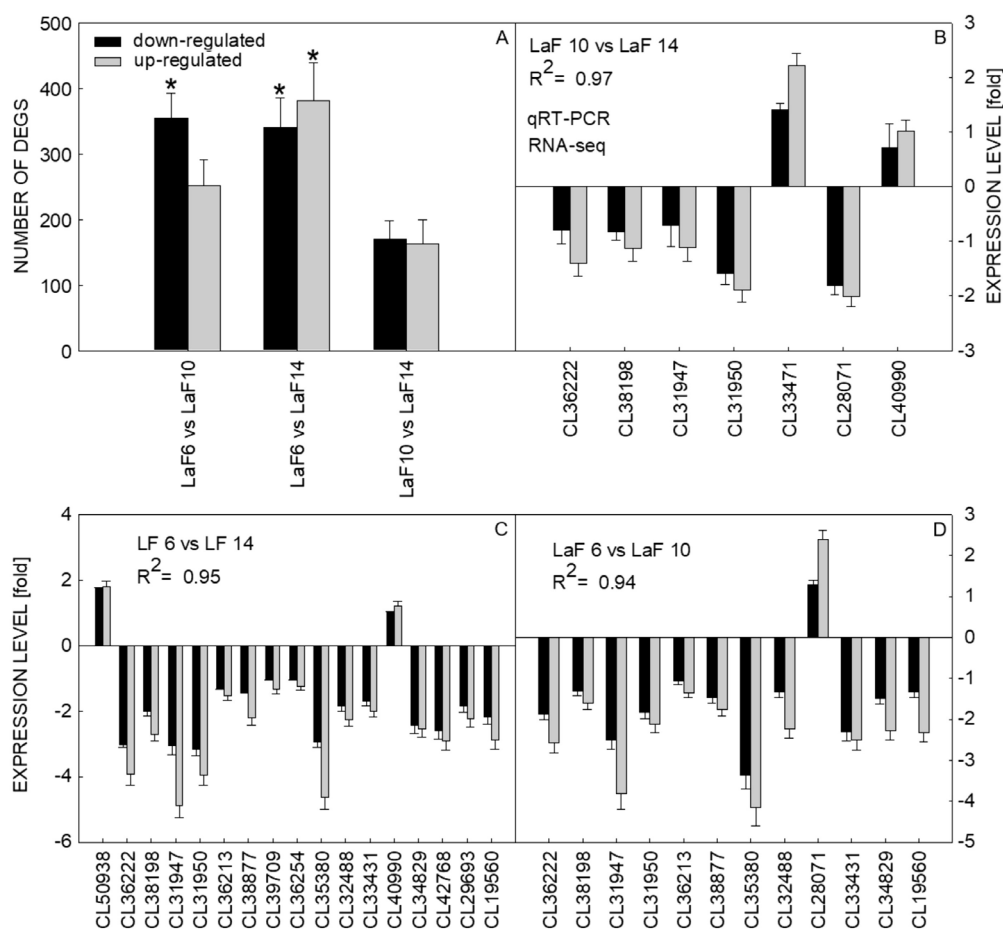


Fig. 3. Gene expression comparisons and RT-qPCR verification. *A* - changes in gene expression profile, the number of up-regulated and down-regulated genes between LF6, LF10, LF14, *B* - RT-qPCR verification of DEGs between LaF10 and LaF14, *C* - RT-qPCR verification of DEGs between LaF6 and LaF14, *D* - RT-qPCR verification of DEGs between LaF6 and LaF10. Means \pm SEs, $n = 3$; significantly different values are denoted by asterisk. LaF6 - 6 florets per flower whorl, LaF10 - 10 florets per flower whorl, LaF14 - 14 florets per flower whorl.

the main DEGs enrichment pathways (Fig. 6 Suppl.). We performed further DEGs enrichment analysis for hormones, and found that 19 DEGs were significantly enriched in the carotenoid biosynthesis pathway, and the difference in the transcription of these 19 genes increased with the increase in floret numbers of inflorescence in lavender, that is,

the more florets, the higher the expressions. In addition, 4 DEGs were significantly enriched in the phenylalanine metabolism pathway, and the difference in the expressions of these 4 genes decreased with the increase in floret numbers of inflorescence in lavender (Fig. 4).

Hormone content analysis showed that the difference

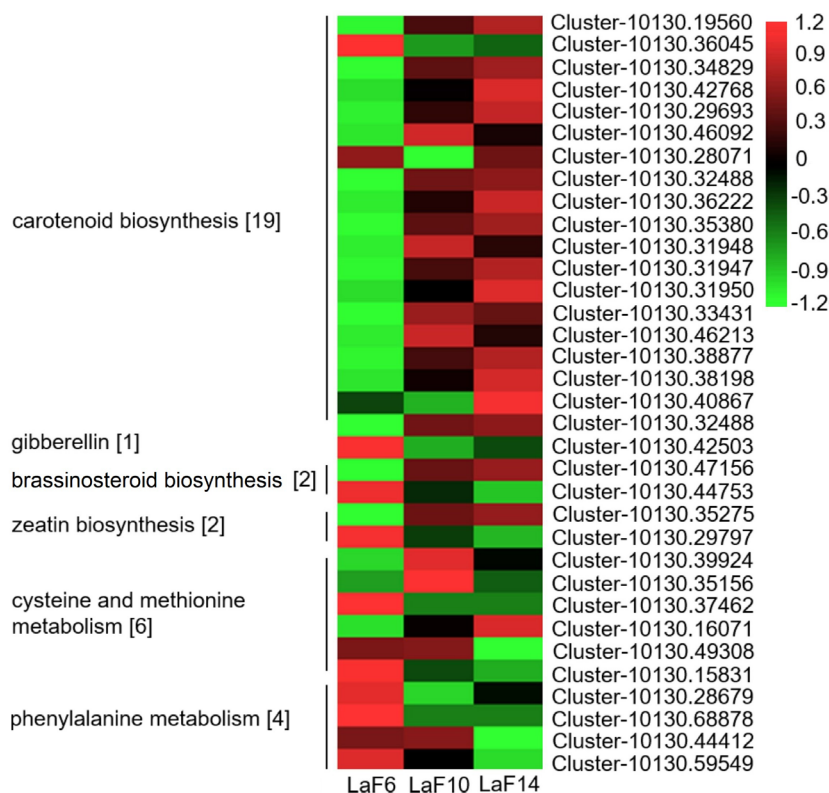


Fig. 4. DEG gene enrichment analysis. Means \pm SEs, $n = 3$. LaF6 - 6 florets per flower whorl, LaF10 - 10 florets per flower whorl, LaF14 - 14 florets per flower whorl.

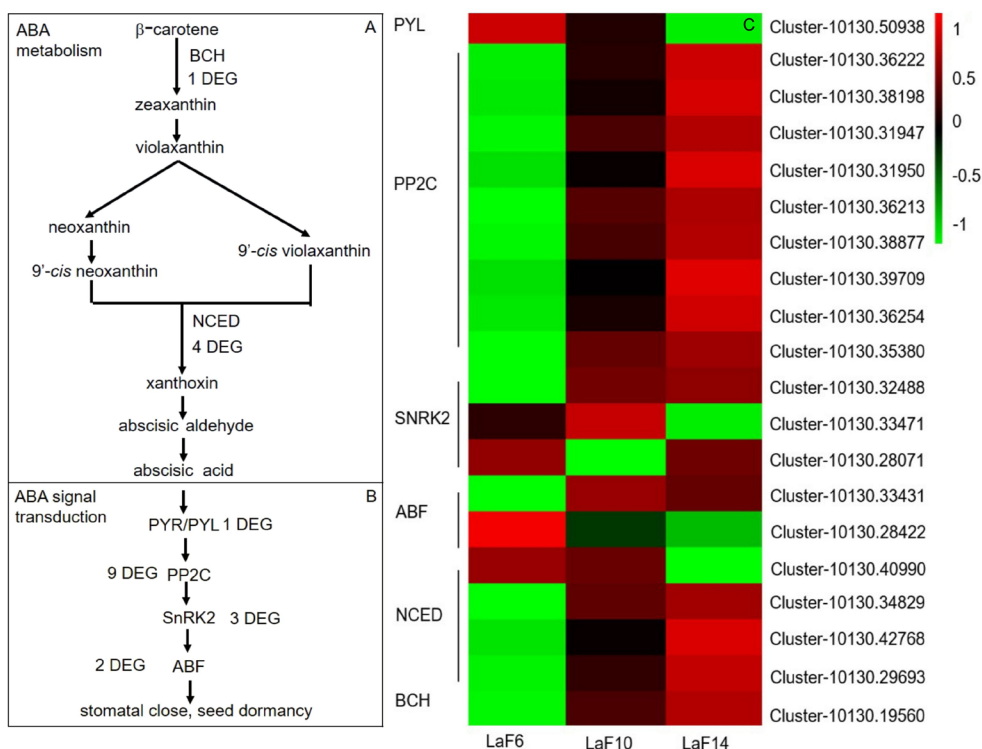


Fig. 5. ABA metabolic pathway and heat map of DEG gene expression in different floret sample. A - the principal pathway of ABA metabolism, B - ABA signal transduction, C - Expression profiles of DEGs involved in different florets. LaF6 - 6 florets per flower whorl, LaF10 - 10 florets per flower whorl, LaF14 - 14 florets per flower whorl.

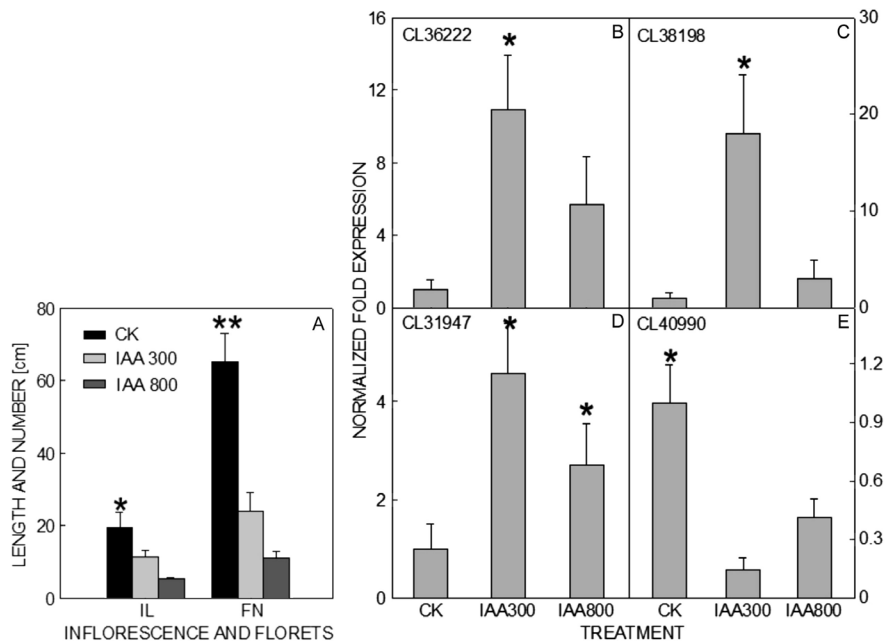


Fig. 6. Effect of IAA application on inflorescence structure (A) and on ABA metabolism key genes (CL36222, CL38198, CL31947, and CL40990) expressions (B-E). IL - inflorescence length, FN - floret number, CK - control, IAA300 - IAA concentration 300 mg·dm⁻³; IAA800 - IAA concentration 800 mg dm⁻³. Means ± SEs, *n* = 3; significantly different values are denoted by asterisk.

in the number of florets was related to ABA metabolism in the flowering axis and axis leaf (Table 1 Suppl., Fig. 2). Here, *KEGG* mapping also found that ABA metabolism (carotenoids biosynthesis pathway) and signaling transduction, IAA signaling transduction was enriched among the different floret samples (Fig. 5). Thus, the DEGs involved in the entire ABA metabolism and signaling transduction were focused.

β -carotene hydroxylase (*BCH*) and 9-*cis*-epoxycarotenoid dioxygenase (*NCED*) were two key enzymes in the ABA biosynthesis pathway, especially the *NCED* (Fig. 5A). The expression of *BCH* gene (CL-10130.19560) in LaF6 sample was lower than that in LaF10 and in LaF14 sample it was the highest (Fig. 5C). Four DEGs encoding *NCED* were found among the floret different samples. Based on their expression pattern, three genes (CL-10130.29693, CL-10130.42768, CL-10130.34829) had similar expression patterns with *BCH* gene, and one gene (CL-10130.40990) had lowest expression in LaF14, and similar in LaF6 and LaF10 samples (Fig. 5C). Above all, the expressions of five ABA biosynthetic genes except one increased with floret numbers together with increasing ABA content.

In the ABA signaling transduction (Fig. 5B), one *PYL* gene, nine *PP2C* genes, three *SnRK2* genes, and two *ABF* genes were found in response to floret differences (Fig. 5B). The expression of *PYL* gene declined with increasing floret numbers. The nine *PP2C* genes all had a similar expression profile with the highest expression in LaF14, followed by that in LaF10, and the lowest expression in LaF6. However, there were complicated expression patterns for *SnRK2* and *ABF* genes. Some of genes encoding homologous products were upregulated, but others were downregulated in the same sample (Fig. 5B).

In IAA signal transduction pathway, three *AUX/IAA* genes and one *SAUR* gene, were found to respond to florets number differences (Fig. 8 Suppl.). The three *AUX/IAA* genes had a similar expression profile that had highest expression in LaF6, followed by that in LaF10, and lowest expression in LaF14. The *SAUR* gene expression trend is not obvious among the samples.

Positive correlations were identified between *BCH*, *NCED*, *PYL*, *PP2C*, *SnRK2*, and *ABF* genes (Fig. 9A Suppl.). Negative correlations were identified between ABA signal pathway and IAA, such as the correlations coefficients of *BCH*, *NCED*, *ABF* and IAA were -0.741, -0.759 and -1.000.

The relationship between ABA and IAA was further investigated by analyzing the network among three key factors of ABA metabolism pathway *NCED*, *PP2C*, *ABF*, and IAA DEGs (Fig. 9B Suppl.). The expressions of IAA DEGs, *IAA18*, *IAA16*, *SAUR* were negatively related to the key genes of ABA metabolism pathway, especially *IAA18*. The correlation coefficients of *IAA18* with *NCED*, *PP2C* and *ABF* are -0.922, -0.814, and -0.953, respectively (Fig. 9B Suppl.). It is speculated that *IAA18* may be the key factors in the relationship between ABA and IAA.

We examined the effect of exogenous hormones on the number of florets. The results showed that exogenous IAA significantly inhibited the number of florets and the inhibitory effect was concentration-dependent (Fig. 6A). The inflorescence length and floret numbers in 300 mg dm⁻³ and 800 mg dm⁻³ treatments were 11.3 and 24.0, 5.2 and 11.0, respectively (Fig. 6A). Compared to the control, the inflorescence length and floret numbers significantly decreased after IAA treatment (Fig. 6A).

In order to test the results of the correlation analysis and verify the relationship between IAA and ABA, we

examined the effect of exogenous IAA on the expression of key genes of ABA metabolism pathway (Fig. 6). The RT-qPCR results showed that exogenous IAA significantly affected the expression of DEGs in the ABA metabolic pathway, such as the ABA biosynthesis gene *NCED* (CL40990) and signaling transduction gene *PP2C* (CL36222, CL38198) (Fig. 6B-E).

Discussion

Increasing number of florets is a desired target of lavender breeding. Exploring the intrinsic mechanism or influencing factors underlying the differences in the floret numbers were the basis for cultivating multi-flowering cultivars. By deep sequencing and function analysis (Fig. 3, Fig. 6 Suppl.) 1 035 DEGs were revealed and top 20 metabolic pathways and signal transduction pathways. These pathways were involved in photosynthesis, carbon fixation, nitrogen metabolism, plant hormone signal transduction, carotenoid biosynthesis, etc., and the hormone metabolism and transduction pathway were the main DEGs enrichment pathways (Fig. 6 Suppl.). Recent findings from different flowering plants suggested that the comprehensive regulatory factors that control inflorescence structure were more or less related to hormone pathways (Teo et al. 2013, Sun et al. 2021). Thus, we focus on the hormone metabolism and transduction pathway.

Previous studies showed that axillary bud's outgrowth can respond to different radiation quality. ABA regulated stem branching by affecting the accumulation of IAA in the buds (Reddy et al. 2013, Holalu and Finlayson 2017). In our experiment, the IAA content and the expression of DEGs (*IAA18*, *IAA16*, and *SAUR*) were negatively correlated with the floret numbers (Table 1 Suppl., Fig. 8 Suppl.). IAA had been proved to be directly linked to regulation of shoot branching in many plants, such as *Oryza sativa* and *Arabidopsis thaliana* (Ferguson and Beveridge 2009, Yao and Finlayson 2015). The ABA content and key genes of ABA metabolism were positively correlated with the floret numbers, 19 DEGs were significantly enriched in the ABA metabolism and transduction, and the differences in the transcription level coincided with the differences in floret numbers (Table 1 Suppl., Figs. 2 and 4). The ABA content of LaF6 samples was significantly lower than that in LaF14 samples ($P < 0.01$). The expressions of ABA metabolism genes *NCED3* or *NCED1* were consistent with endogenous ABA content, and increased with the number of florets. Previous studies also showed that high expression of *AtNCED3*, *VvNCED1* in *Arabidopsis* and *Vitis vinifera* can significantly increase the content of endogenous ABA (Boyd et al. 2009, Acanda et al. 2020, Baek et al. 2020). It was speculated that ABA was involved in floret numbers regulation also in *L. angustifolia*.

Like ABA metabolic pathways, some components of ABA signaling transduction were also different among LaF6, LaF10, and LaF14 samples, such as the proteins PYR/PYL, PP2C, SnRK2, and ABF. These core component proteins constituted a dual negative regulatory system that regulates ABA signaling (Raghavendra et al. 2010, Cutler

et al. 2010, Hu et al. 2012). Previous studies showed that seed germination, vegetative growth, and stomatal movements were more sensitive to ABA in the plant in which *PYL9/RCAR1*, *PYL5/RCAR8* or *PYL8/RCAR3* genes were over-expressed (Cutler et al. 2010, Hu et al. 2012). In our experiment, PYR/PYL, PP2C, SnRK2 and ABF proteins in LaF6, LaF10, and LaF14 samples aggregated different numbers of DEGs (Fig. 5). Further molecular mechanisms study showed that ABA is involved in the regulation of floret numbers in *L. angustifolia* inflorescence.

ABA has been known as the plant stress hormone. However, it also plays a role in non-stress-related plant development and growth processes. ABA may turn out to be one of the earliest upstream factors when shoot branching responds to environmental signal (Rameau et al. 2015). In our experiment, ABA content is positively correlated with the number of florets, while IAA content is the opposite (Fig. 2). The IAA and ABA content in the LaF6 were 369.2 and 452.6 ng g⁻¹, and it was 90.3 and 4534.5 ng g⁻¹ in the LaF14 sample (Fig. 2). Pot experiment also confirmed that exogenous IAA significantly inhibited the number of florets, and the inhibitory effect was positively related to IAA concentration (Fig. 6). The change of ABA/IAA ratio also correlated with the floret numbers (Fig. 2B). According to phenotypic data, it was speculated that the regulation of ABA on the floret numbers was related to the IAA content.

Correlation analysis showed that the expressions of key genes of ABA metabolism pathway, such as *NCED*, *PYL*, *PP2C*, *ABF*, and *SnRK2* were all negatively correlated with the expressions of IAA genes (Fig. 9A Suppl.). In pot experiments, exogenous IAA could also affect the expression of DEGs in the ABA metabolic pathway (Fig. 6B-E). Further correlation analysis between the ABA metabolic factors and the IAA DEGs (*IAA18*, *IAA16*, and *SAUR*) showed that *IAA18* have a negative correlation with the ABA metabolism genes (*NCED*, *PP2C*, *ABF*) (Fig. 9B Suppl.). Previous studies had proved that *IAA18* was mainly involved in the regulation of plant axillary meristems development (Uehara et al. 2008, Bustillo-Avendano et al. 2018). The characteristics of verticillaster inflorescence indicated that the key factors affecting the number of JX-2 florets were the axillary meristems and their branching (Fig. 1). *IAA18* may be a keystone in the interaction between ABA and IAA.

Previous studies also showed that ABA and IAA interacted with each other in many developmental processes, especially, in the regulating root growth, seed vigor, etc. (Brady et al. 2003, Emenecker and Strader 2020, Ge et al. 2020, Zhou et al. 2020). ABA also regulated lateral root formation and elongation by suppressing the expression of *PIN-FORMED1* through the protein ABA-insensitive (*ABI4*) (Brady et al. 2003). In *Populus*, *PdNF-YB21* positively regulates root growth and drought resistance by ABA mediated IAA transport (He et al. 2020).

Conclusions

Comprehensive analysis of previous research and our experimental results showed that ABA may affect the IAA transport and accumulation which leads to axillary meristems increase and the floret number differences. The reason for the difference of floret numbers in the lavender clusters may be different ABA content in floral axis leaf in the flower bud stage. The *IAA18* gene was the keystone in ABA interaction with IAA.

References

- Acanda, Y., Martí, Ó., Prado, M.J., González, M.V., Rey, M.: Changes in abscisic acid metabolism in relation to the maturation of grapevine (*Vitis vinifera* L., cv. Mencía) somatic embryos. - *BMC Plant Biol.* **20**: 487, 2020.
- Baek, D.W., Kim, W.Y., Cha, J.Y., Park, H.J., Shin, G., Park, J.H., Lim, C.J., Chun, H.J., Li, N., Kim, D.H., Lee, S.Y., Pardo, J.M., Kim, M.C., Yun, D.J.: The GIGANTEA-enhanced EM level complex enhances drought tolerance *via* regulation of abscisic acid synthesis. - *Plant Physiol.* **184**: 443-458, 2020.
- Boyd, J., Gai, Y.Z., Nelson, K.M., Lukiwshi, E., Talbot, J., Loewen, M.K., Owen, S., Zaharia, L.L., Cutler, A.J., Abrams, S.R., Loewen, M.C.: Sesquiterpene-like inhibitors of a 9-*cis*-epoxycarotenoid dioxygenase regulating abscisic acid biosynthesis in higher plants. - *Bioorgan. med. Chem.* **17**: 2902-2912, 2009.
- Brady, S.M., Sarkar, S.F., Bonetta, D., McCourt, P.: The *ABSCISIC ACID INSENSITIVE 3 (ABI3)* gene is modulated by farnesylation and is involved in IAA signaling and lateral root development in *Arabidopsis*. - *Plant J.* **34**: 67-75, 2003.
- Bustillo-Avendano, E., Ibáñez, S., Sanz, O., Sousa-Barros, J.A., Gude, I., Perianez-Rodriguez, J., Micol, J.L., Del-Pozo, J.C., Moreno-Risueno, M.A., Pérez-Pérez, J.M.: Regulation of hormonal control, cell reprogramming and patterning during *de novo* root organogenesis. - *Plant Physiol.* **176**: 1709-1727, 2018.
- Cheng, Y.F., Dai, X.H., Zhao, Y.D.: Auxin synthesized by YUCCA flavin monooxygenases is essential for embryogenesis and leaf formation in *Arabidopsis*. - *Plant Cell* **19**: 2430-2439, 2007.
- Conesa, A., Götz, S., García-Gómez, J.M., Terol, J., Talón, M., Robles, M., Montserrat, R.: *Blast2GO*: a universal tool for annotation, visualization and analysis in functional genomics research. - *Bioinformatics* **21**: 3674-3676, 2005.
- Cutler, S.R., Rodriguez, P.L., Finkelstein, R.R., Abrams, S.R.: Abscisic acid: emergence of a core signaling network. - *Annu. Rev. Plant Biol.* **61**: 651-679, 2010.
- Emenecker, R.J., Stader, L.C.: Auxin-abscisic acid interactions in plant growth and development. - *Biomolecules* **10**: 281, 2020.
- Ferguson, B.J., Beveridge, C.A.: Roles for auxin, cytokinin, and strigolactone in regulation shoot branching. - *Plant Physiol.* **149**: 1929-1944, 2009.
- Ge, W.J., Bu, H.Y., Wang, X.J., Xia, Y.B., Shantel, A.M., Wang, X.T., Qi, W., Liu, K., Du, G.Z.: Changes in endogenous hormone contents during seed germination of *Anemone rivularis* var. *flore-minore*. - *GECCO* **24**: e01200, 2020.
- Grabherr, M.G., Haas, B.J., Yassour, M., Levin, J.Z., Thompson, D.A., Amit, I.: Full-length transcriptome assembly from RNA-Seq data without a reference genome. - *Nat. Biotechnol.* **29**: 644-652, 2011.
- Han, Y.Y., Yang, H.B., Jiao, Y.L.: Regulation of inflorescence architecture by cytokinins. - *Front. Plant Sci.* **5**: 669, 2014.
- He, Y.Q., Zhao, J., Yang, B., Sun, S., Peng, L.L., Wang, Z.F.: Indole-3-acetate beta-glucosyltransferase OsIAGLU regulates seed vigour through mediating crosstalk between auxin and abscisic acid in rice. - *Plant Biotechnol. J.* **18**: 1933-1945, 2020.
- Holalu, S.V., Finlayson, S.A.: The red light:far red light alters *Arabidopsis* axillary bud growth and abscisic acid signaling before stem auxin changes. - *J. exp. Bot.* **67**: 943-952, 2017.
- Hu, S., Wang, F.Z., Liu, Z.N., Liu, Y.P., Yu, X.L.: ABA signaling mediated by PYR/PYL/RCAR in plants. - *Hereditas* **34**: 560-572, 2012.
- Kanehisa, M., Goto, S., Sato, Y., Furumichi, M., Tanabe, M.: *KEGG* for integration and interpretation of large-scale molecular datasets. - *Nucl. Acids Res.* **40**: 109-114, 2012.
- Li, H., Li, J.R., Dong, Y.M., Hao, H.P., Bai, H.T., Wang, H.F., Cui, H.X., Shi, L.: Time-series transcriptome provides insights into the gene regulation network involved in the volatile terpenoid metabolism during the flower development of lavender. - *BMC Plant Biol.* **19**: 313, 2019.
- McSteen, P.: Hormonal regulation of branching in grasses. - *Plant Physiol.* **149**: 46-55, 2009.
- Müller, A., Dücking, P., Weiler, E.W.: A multiplex GC-MS/MS technique for the sensitive and quantitative single-run analysis of acidic phytohormones and related compounds, and its application to *Arabidopsis thaliana*. - *Planta* **216**: 44-56, 2002.
- Murphy, A.: Hormone crosstalk in plants. - *J. exp. Bot.* **66**: 4853-4854, 2015.
- Ongaro, V., Leyser, O.: Hormonal control of shoot branching. - *J. exp. Bot.* **59**: 67-74, 2008.
- Raghavendra, A.S., Gonugunta, V.K., Christmann, A., Grill, E.: ABA perception and signaling. - *Trends Plant Sci.* **15**: 395-401, 2010.
- Rameau, C., Bertheloot, J., Leduc, N., Andrier, B., Foucher, F., Sakr, S.: Multiple pathways regulate shoot branching. - *Front. Plant Sci.* **5**: 1-15, 2015.
- Reddy, S.K., Holalu, S.V., Casal, J.J., Finlayson, S.A.: Abscisic acid regulates axillary bud outgrowth responses to the ratio of red to far-red light. - *Plant Physiol.* **163**: 1047-1058, 2013.
- Sun, Q., Xie, Y., Li, H., Liu, J., Geng, R., Wang, P., Chu, Z.Y., Chang, Y., Li, G.J., Zhang, X., Yuan Y.L., Cai, Y.F.: Cotton *GhBRC1* regulates branching, flowering, and growth by integrating multiple hormone pathways. - *Crops J.* **10**: 75-87, 2021.
- Tatusov, R.L., Natale, D.A., Garkavtsev, I.V., Tatusova, T.A., Shankavaram, U.T., Rao, B.S., Kiryutin, B., Galperin, M.Y., Fedorova, N.D., Koonin, E.V.: The *COG* database: new development sinphylogenetic classification of proteins from complete genomes. - *Nucl. Acids Res.* **29**: 22-28, 2001.
- Teo, Z.W.N., Song, S., Wang, Y.Q., Liu, J., Yu, H.: New insights into the regulation of inflorescence architecture. - *Trends Plant Sci.* **19**: 158-165, 2013.
- Uehara, T., Okushima, Y., Mimura, T., Tasaka, M., Fukaki, H.: Domain II mutations in *CRANE/IAA18* suppress lateral root formation and affect shoot development in *Arabidopsis thaliana*. - *Plant Cell Physiol.* **49**: 1025-1038, 2008.
- Wu, X.T., McSteen, P.: The role of auxin transport during inflorescence development in maize (*Zea mays*, *Poaceae*). - *Amer. J. Bot.* **94**: 1745-55, 2007.
- Xie, Q., Essemine, J., Pang, X., Chen, H., Jin, J., Cai, W.: Abscisic acid regulates the root growth trajectory by reducing auxin transporter PIN2 protein levels in *Arabidopsis thaliana*. - *Front. Plant Sci.* **12**: 632676, 2021.
- Yang, J., Zhang, J., Wang, Z., Zhu, Q., Liu, L.: Water deficit

- induced senescence and its relationship to the remobilization of pre-stored carbon in wheat during grain filling. - *Agron. J.* **93**: 196-206, 2001.
- Yao, C., Finlayson, S.A.: Abscisic acid is a general negative regulator of *Arabidopsis* axillary bud growth. - *Plant Physiol.* **169**: 611-626, 2015.
- Zai, X.: Study on the Dynamic Growth and Components Accumulation of *Lavandula angustifolia* Master. - Henan Agricultural University, Zhengzhou 2011.
- Zhou, Y.Y., Zhang, Y., Wang, X.W., Han, X., An, Y., Lin, S.W., Chao, S., Wen, J.L., Liu, C., Yin, W.L., Xia, X.L.: Root-specific NF-Y family transcription factor, PdNF-YB21, positively regulates root growth and drought resistance by abscisic acid-mediated indoleacetic acid transport in *Populus*. - *New. Phytol.* **227**: 407-426, 2020.